Ecological Modelling 464 (2022) 109815

Contents lists available at ScienceDirect

Ecological Modelling

journal homepage: www.elsevier.com/locate/ecolmodel

Quantifying the GCM-related uncertainty for climate change impact assessment of rainfed rice production in Cambodia by a combined hydrologic - rice growth model

K. Tsujimoto [a,*], N. Kuriya [b], T. Ohta [c], K. Homma [d], M.So Im [e]

[a] Graduate School of Environmental and Life Science, Okayama University, 3-1-1 Tsushima-naka, Kita-ku, Okayama, 700-8530, Japan
[b] Faculty of Environmental Science and Technology, Okayama University, 3-1-1 Tsushima-naka, Kita-ku, Okayama, 700-8530, Japan
[c] Assistance Unit for Research and Engineering Development (U-PRIMO). Kita-ku, Okayama 700-0085, Japan
[d] Graduate School of Agricultural Science, Tohoku University, 468-1 Aramaki Aza Aoba, Aoba-ku, Sendai 980-8572, Japan
[e] Ministry of Water Resources and Meteorology (MOWRAM) of Cambodia. 364 Monivong Boulvard Sangkat Psar Deumthkov Khan Chamkar Morn, Phnom Penh, Cambodia

ARTICLE INFO

Keywords:
Climate change impact assessment
Soil moisture
Crop model
Rice production
Rainfed paddy
GCM

ABSTRACT

The effects of climate change on agriculture are a major concern for global food security. In this study, the impacts of climate change on rainfed rice production in the granary of Cambodia were examined on a basin scale by developing and applying a combined model consisting of a crop model and a basin-scale distributed hydrological model. The response of rice production to soil-water availability was simulated for past (1981–2000) and future (2041–2060, 2081–2100) periods. From 34 general circulation models (GCMs) that participated in the Coupled Model Intercomparison Project Phase 5 (CMIP5), 5 GCMs were selected by evaluating monthly rainfall in the past. Although annual rainfall was projected to increase by all five selected GCMs, notable decreases in rainfed rice production were projected with 3 GCMs, while small changes were projected with the other 2 GCMs. The main factor restricting future rice production was soil water availability, brought by the projected change in the seasonal distribution of rainfall and the projected more severe dry spells in the early monsoon season. The results suggest the importance of the selection and bias correction of GCMs to force rice crop models and of the simulation of soil water flow on a basin scale for the assessment of rain-fed rice production. In particular, improvements in projections of rainfall amounts over shorter periods rather than annual or seasonal periods, which fit within the time scales of rice plant growth, were suggested to be important.

Abbreviations

APHRODITE: Asian Precipitation – Highly Resolved Observational Data Integration Towards Evaluation of Water Resources
CMIP5: Coupled Model Intercomparison Project Phase 5
DIAS: Data Integration and Analysis System
GCM: General Circulation Model
GPCP: Global Precipitation Climatology Project
IDW: Inverse Distance Weight
JRA-55: The Japanese 55-year Reanalysis
LAI: Leaf Area Index
MODIS: Moderate Resolution Imaging Spectroradiometer
RCP: Representative Concentration Pathway
RMSE: Root Mean Square Error
SCORR: Spatial CORRelation coefficient
SiB2: Simple Biosphere model 2
WEB-DHM: Water and Energy Budget-based Distributed Hydrological Model

1. Introduction

The Fifth Assessment Report (AR5) of the Intergovernmental Panel on Climate Change (IPCC) states that multidecadal global warming since the 1950s is unequivocal (IPCC, 2014). The Sixth Assessment Report (AR6) is currently under preparation to be released between 2021 and 2022, and public concern about the impact of climate change is arising. Climate change has severely affected many agricultural regions and is one of the major concerns for global food security, as it restricts stable

* Corresponding author.
E-mail address: tsujimoto@okayama-u.ac.jp (K. Tsujimoto).

https://doi.org/10.1016/j.ecolmodel.2021.109815
Received 13 May 2021; Received in revised form 3 November 2021; Accepted 5 November 2021
Available online 17 November 2021

crop production (McLaughlin and Kinzelbach, 2015). The negative impacts of climate change on agriculture are considered more serious in tropical developing countries because frequent heat stress and drought are combined with low levels of technological development (Li et al., 2017).

Cambodia is a developing country located in the Lower Mekong River basin on the Indochina Peninsula. It relies heavily on agriculture for its economic development; more than half of the total workforce is engaged in agriculture, and agriculture contributed approximately 32% of the national gross domestic product (GDP) as of 2011 (National Climatic Change Committe, 2013). Irrigation rates remain low, at approximately 12% of the cropland (Mekong River Commission, 2018), and most crops are rainfed. Accordingly, a change in rainfall under climate change is a great threat to agricultural management, crop production, and socioeconomic activity in Cambodia. With increasing demand for agricultural products from the Lower Mekong River basin, sustaining and improving rice production under climate change is key for the development of the country. A quantitative impact assessment of climate change on rice production is essential for informing policies on adaptation strategies, including investment in irrigation facilities and other agricultural infrastructure. Given the increasing socioeconomic need in Cambodia for agricultural management under climate change, this study carries out an impact assessment on rainfed paddy rice production in Cambodia.

Among various climatic factors, rainfall, temperature, solar radiation, and CO_2 concentration are the most important climate factors affecting crop productivity (Li et al., 2017). There are many studies dealing with the effects of increasing CO_2, and they show clear evidence that when interactions with other climate variables are ignored, more CO_2 leads to higher crop yields (Ainsworth and Long, 2005; Kim et al., 2003; Kimball et al., 2002) because of enhanced photosynthesis. In more realistic studies, however, higher air temperatures from elevated CO_2 levels tend to suppress the increase in yield (Krishnan et al., 2007). For rice, a rise in air temperature is generally considered to decrease yield because of the lower spikelet fertility (Prasad et al., 2006) as well as the higher evaporative demand of the crop (Deb et al., 2016). Because of such interactions of various climatological factors, the IPCC AR5 (IPCC, 2014) reports high variability in the projected changes in rice production under climate change.

Recent studies on biophysical process-based rice crop modeling include the applications and developments of SIMRIW (Horie et al., 1992, 1995), ORYZA2000 (Bouman et al., 2001), the CERES-Rice model (Mahmood, 1998) of the Decision Support System for Agrotechnology Transfer (DSSAT) (Jones et al., 1998), and AquaCrop (Steduto et al., 2009). These models are designed to simulate rice plant growth, including photosynthesis, respiration, leaf area development, dry matter accumulation, phenological development, and yield, through simulations of the water and nitrogen balance in the soil accounting for the effects of the temperature and CO_2 concentration in the atmosphere. Crop details, soil properties, weather conditions, and rice management practices are the main inputs to drive these models. Each of these models has a series of developmental varieties in their modules and has been applied to climate change impact studies by many researchers worldwide. SIMRIW-rainfed selected for this study was derived from SIMRIW to simulate rice plant growth under limited conditions for water and nitrogen (Homma and Horie, 2009; Ohnishi et al., 1997). The model was validated in Thailand and Indonesia (Homma and Horie, 2009; Homma et al., 2017b), and its modified version for remote sensing was also validated in Thailand and Lao PDR (Maki et al., 2017; Raksapatcharawong et al., 2020). However, these abovementioned rice crop models, including SIMRIW-rainfed model, are developed on a point-scale basis without consideration of the basin-scale hydrological cycle and its associated soil-water flow in the basin, although water availability is the most important factor for rain-fed rice production.

For predicting the global climate, GCMs are the primary tools, and many studies have used GCMs with rice crop models to assess the potential effects of climate change on rice production. Impact assessments of rice production based on multimodel ensemble projections using the GCMs included in CMIP5 (Taylor et al., 2012) have been conducted in many areas in the world, including Iran (Darzi-Naftchali and Karandish, 2019), China (He et al., 2018; Zhang et al., 2019a; Zheng et al., 2020), Vietnam (Deb et al., 2016), and Thailand (Arunrat et al., 2018; Boonwichai et al., 2019). However, uncertainty in GCM projections of soil moisture over monsoon regions is reported to be higher than that of other variables because of the diverse soil schemes and vegetation parameterizations in GCMs (Zhang et al., 2019b). Thus, the effect of soil moisture stress can be largely dependent on the selection of the GCMs to be used as inputs to the rice model. The selection of the GCMs and the GCM-related uncertainties have not been, however, paid enough attention in earlier studies in applying rice models for climate change impact assessments.

The uncertainties in projected rice production can therefore be larger for rain-fed paddies. While many of the earlier studies assessing climate change impacts on crop production assumed irrigated conditions with high soil-water availability, the potential effects of water stress on rainfed paddies have not been well examined (Babel et al., 2011), despite the prevalence of rainfed paddies in many developing countries and the knowledge that water stress (drought) is one of the main factors restricting rice production (Homma et al., 2004; Prabnakorn et al., 2018).

In assessing rain-fed rice production, the daily evolution of soil moisture in the growing season is key to assessing the water-stress impact on rice growth and yield; therefore, precipitation, radiation, and air temperature need to be appropriately given from the GCMs to the rice model to simulate the actual evapotranspiration in the limited condition of soil water. In this regard, the evaluation and selection of GCMs in terms of reproducibility on a daily scale should be examined carefully, while many earlier studies pay little attention to them and are mainly based on monthly reproducibility. Although increases in soil moisture were projected in earlier studies in the Asian monsoon region for India (Saseendran et al., 2000) and the Yangtze River basin in China (Sun et al., 2019), our hypothesis is that the drought effect on rain-fed rice production can be highly affected by the finer time-scale distributions of rainfall and soil moisture, and thus drought can be more severe even under the increased rainfall amount over a time period from several months to a year.

For reliable projections of soil moisture and rainfed rice production, it is considered more effective to simulate the soil-water flow with vegetation effects at higher spatiotemporal resolution instead of directly using the GCM outputs. In this study, we thus developed and applied a combined hydrologic and crop (rice) model, which is named “mizuha”, to concurrently simulate horizontal and vertical soil-water flows based on the basin-scale hydrologic cycle and the growth and yield of rice in response to root-zone soil moisture.

By developing the research methodology framework to select the “best” GCMs to be used for rain-fed rice production assessment and to use the combined hydrologic-rice growth model, we quantified the GCM-related uncertainty in assessing the impact of climate change on rain-fed rice production where soil moisture plays a key role. With this study, we aim to provide suggestions to the scientific community for future improvement of the GCM from the viewpoint of simulating rain-fed rice production and to provide information for local policy makers in Cambodia for climate change adaptation.

2. Materials and methods

In this study, rain-fed rice production in Cambodia under future climates was assessed. The overall procedure and the scientific questions to be solved in this study are conceptually described in Fig. 1. This study is unique in that future rice production is assessed not on a point scale but on a basin scale by combining hydrologic and rice growth models to improve the simulation accuracy of soil moisture and soil-water stress to

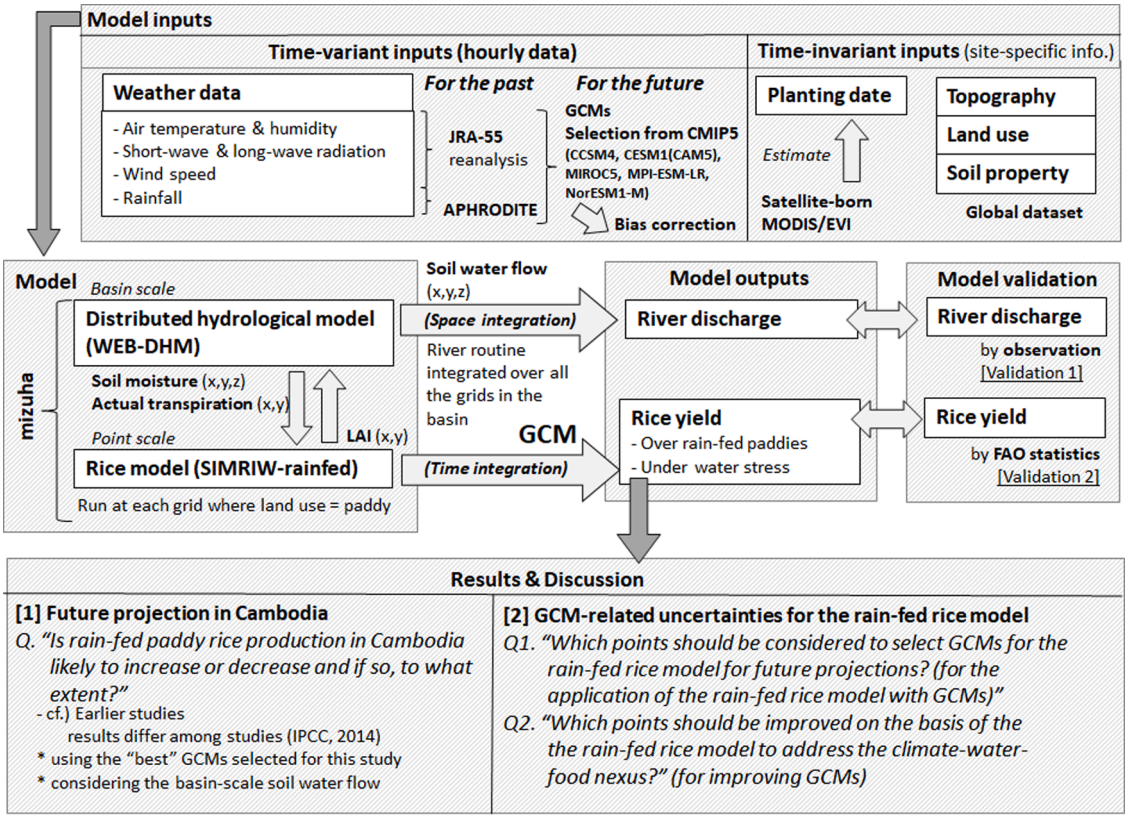

Fig. 1. Diagram of the overall methodology in this study.

rice growth under nonirrigated conditions. In addition, it is notable that the selection and bias correction methods of the GCMs have been deeply examined to be properly given to the rice growth model in the context of obtaining climatic variables with their time series that affect rice growth. The detailed procedures are shown in the following sections.

2.1. Study area

The Pursat River basin in western Cambodia (Fig. 2a and b) was selected as the study area. Its watershed area is approximately 6760 km^2, and it runs from southwest to northeast to flow into Tonle Sap Lake. Based on the elevation data from the Advanced Spaceborne Thermal Emission and Reflection Radiometer (ASTER) (NASA, 2020), nine main subbasins were defined by the Pfafstetter algorithm (Yang et al., 2002), as indicated in Fig. 2b, with odd subbasin numbers (1, 3, 5, 7, 9) along the main stream and even numbers (2, 4, 6, 8) for tributaries.

The land-use distribution (Fig. 2c) was obtained from the U.S. Geological Survey global data (Global Land Cover Characterization version 1.2; USGS, 2020a) and all the cropland in the middle-to-lower basin (1396 km^2) was assumed to be paddy, since the authors observed the prevalence of paddy fields through the middle-to-lower basin with other crop types distributed mainly in the upper basin. Another correspondence table for the original USGS categorization and the model application in this study is shown in Table S1 of the Supplementary Material. The soil types and their properties, including the van Genuchten parameters, are given by the Food and Agriculture Organization (FAO, 2007) (Fig. 2d and Table 1).

2.2. Rice growth model (SIMRIW-rainfed)

The SImulation Model for RIce-Weather relations (SIMRIW)-rainfed (Homma and Horie, 2009) was applied in this study to simulate the growth and yield of rice plants. SIMRIW-rainfed is based on SIMRIW (Horie et al., 1992, 1995) with additional components to include water stress effects on rice plants.

Phenological development is based on SIMRIW (Horie et al., 1992, 1995) and is described with the developmental index (DVI), for which its value is defined as 0 for seeding emergence, 1 for heading, and 2 for maturity. The DVI is calculated as the integration of the daily developmental rate (DVR)

$$DVI = \sum DVR \tag{1}$$

The leaf area index (LAI, *lai*), aboveground dry matter (*dm*), and grain yield (*yield*) are represented as

$$lai = f_1(RER_{max},\ RDR,\ T_{air},\ \Delta nup,\ ws, DVI) \tag{2}$$

$$dm = f_2(RCE,\ S_d,\ T_{air}, lai,\ \Delta nup,\ ws) \tag{3}$$

$$yield = f_3(dm,\ HI,\ nup,\ ws,\ DVI) \tag{4}$$

where RER_{max} is the maximum relative expansion rate of LAI, *RDR* is the relative leaf death rate, *RCE* is the radiation conversion efficiency, and *HI* is the harvest index. T_{air} and S_d are air temperature and solar radiation, respectively, and are given through the hydrological submodel (WEB-DHM) to SIMRIW-rainfed in the model. *nup* and *ws* are plant nitrogen uptake and water stress, respectively, and are given with the following equations.

$$\Delta Npool = f_4(T_{air},\ smc,\ fertilizer,\ nup) \tag{5}$$

$$\Delta nup = f_5(Npool,\ ws,\ DVI) \tag{6}$$

$$ws = \sum_{DVI=0} f_6(swc) \tag{7}$$

where *Npool* is the available nitrogen in the soil, *fertilizer* is the fertilizer application amount, and *swc* is the root-zone soil moisture, which is

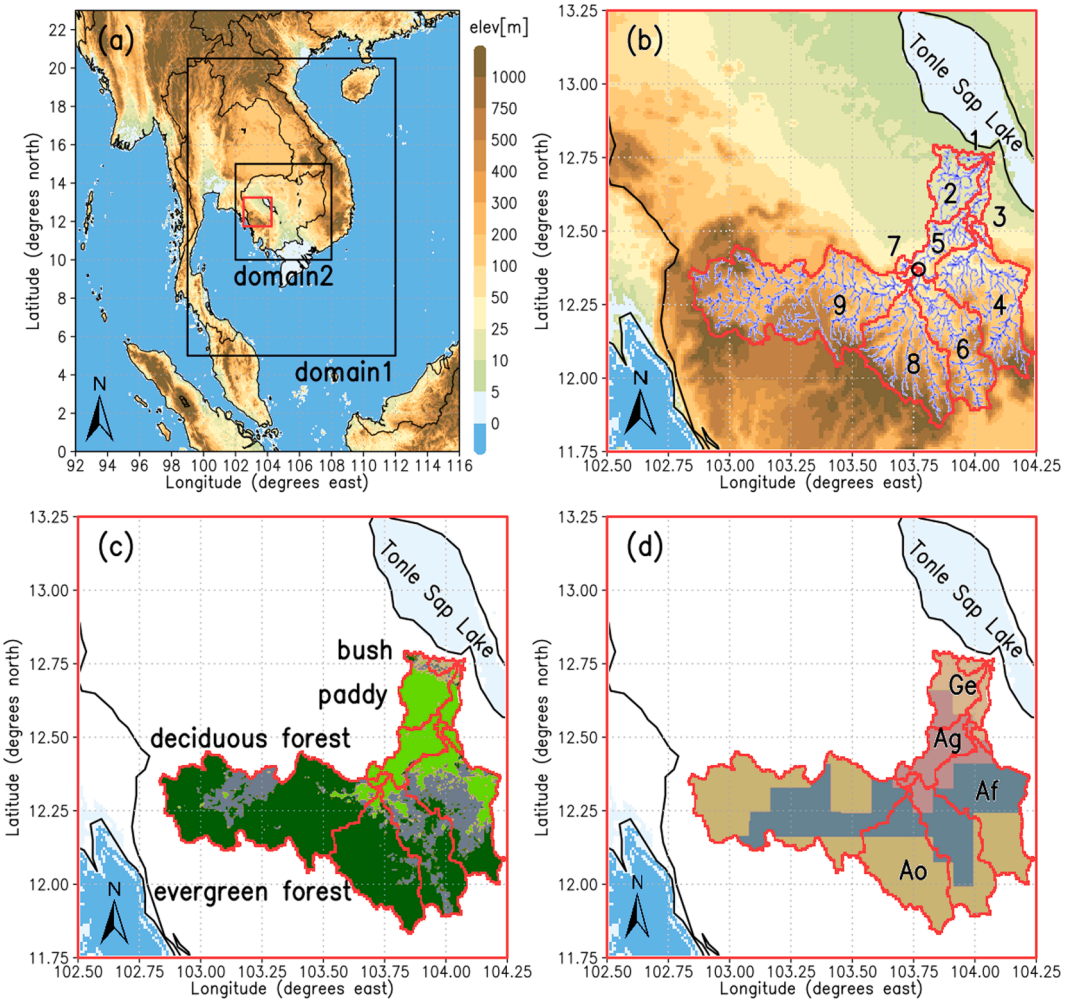

Fig. 2. Study Area. (a) Regional map of the Indochina Peninsula and Cambodia. The black rectangular areas indicate the two domains for the GCM evaluation (domain 1 represents the Indochina Peninsula, and domain 2 represents Cambodia). The red rectangular area includes the Pursat River basin and is the same area shown in (b)–(d). (b) Location of the Pursat River basin shown with its river channels, main subbasins, and the location of river discharge observations (○) that were considered in the model simulation. (c) Land-use types from the USGS global data with modifications. (d) Distribution of the soil types (Eutric Gleysol (Ge), Gleyic Acrisols (Ag), Ferric Acrisols (Af), and Orthic Acrisols (Ao)) from the FAO global data.

Table 1
Soil types in the study area and their van Genuchten parameters (saturated water content θ_{sat}, residual water content θ_{rsd}, and parameters α and n).

Soil Type	Sand [%]	Silt [%]	Clay [%]	α [kPa^{-1}]	n [-]	θ_{sat} [m^3 m^{-3}]	θ_{rsd} [m^3 m^{-3}]
Eutric Gleysol (Ge)	43	20	37	0.15	1.435	0.456	0.082
Gleyic Acrisols (Ag)	41	27	32	0.22	1.524	0.448	0.069
Ferric Acrisols (Af)	62	14	24	0.25	1.592	0.452	0.073
Orthic Acrisols (Ao)	54	16	31	0.22	1.539	0.451	0.071

Source: FAO (2007).

calculated in WEB-DHM in this study. The water stress is calculated as the accumulated values from the initiation of the growth. Following SIMRIW-rainfed, the effect of *ws* is considered in the calculation of *DVR* as well.

Although many factors change from present to future and affect rice production, we considered only meteorological factors such as rainfall (through *swc*), T_{air}, and S_d for the changes. It was assumed that no changes would occur in other factors, including CO_2 concentration, fertilizer, irrigation, and rice cultivars, and the same values were used in all the past and future simulations. The CO_2 concentration was set to 370 ppm. The parameters that were calibrated for rainfed rice in northeast Thailand were used, but the phenological development of rice cultivars and farmer management were adjusted to approximate the conditions in Cambodia in 2013–2014 (Hirooka et al., 2016; Kodo et al., 2021). Damage by pests and diseases was not considered, and only the damage brought by water stress was evaluated to highlight the hydrological restriction on rain-fed rice production in this region. Only single cropping in the rainy season under rainfed conditions without irrigation was considered.

2.3. Combined hydrologic-rice growth model (mizuha)

The combined SIMRIW rainfed model with a hydrological model was applied in this study to hourly simulate the concurrent responses of the basin-scale hydrologic cycle and rice growth with consideration of soil water flow in the basin and improved soil moisture estimation. For the

hydrologic model, the Water and Energy Budget-based Distributed Hydrological Model (WEB-DHM) (Wang et al., 2009b) was used. The WEB-DHM is based on the Geomorphology-Based Hydrological Model (GBHM) (Yang et al., 2002) and is characterized by the incorporation (Wang et al., 2009a) of the modified Simple Biosphere model 2 (SiB2) (Sellers et al., 1996) to realize a process-based description for evapotranspiration considering the water and energy fluxes from the land surface and soil-water flow. The combined model of WEB-DHM and SIMRIW-rainfed is named "mizuha" in this study and was previously used for climate change impact assessment in Cambodia with CMIP3 data (SoSo Im et al., 2014) and in Indonesia with CMIP5 data (Homma et al., 2017a).

For WEB-DHM application, the target basin was divided into 500 m × 500 m square grids in which soil-water flow was calculated by the Richards equation (Richards, 1931), considering the soil-water retention characteristics modeled by van Genuchten (van Genuchten, 1980). In paddy grids, the root-zone depth was set to 50 cm and vertically discretized into 5 cm sublayers in the root zone and 10 cm sublayers below the root zone for soil-water flow simulation. The hillslope flow and subsurface flow from the grids were integrated for each flow interval in a subbasin to obtain river discharge.

The root-zone soil moisture calculated in WEB-DHM was put into SIMRIW-rainfed paddy grids at each time step to simulate water stress and rice plant growth. The LAI expansion was simulated by SIMRIW-rainfed in response to water stress and was returned to WEB-DHM to be used for the hydrologic simulation in the next time step. In WEB-DHM, the LAI is used together with the fraction of photosynthetically active radiation (FPAR) to simulate canopy interception, transpiration, and surface energy budget. Except for paddy grids for which the LAI simulated by SIMRIW-rainfed grids is passed to WEB-DHM, the 8-day composites of LAI and FPAR from the Moderate Resolution Imaging Spectroradiometer (MODIS) onboard the Terra and Aqua satellites (MCD15A2H v006 product) (USGS, 2020d) are used. Because of the limited period (2003–present) of data availability for the LAI and FPAR from Terra/Aqua MODIS, the data from 2003 and 2019 were used in all the years in the past and future runs, respectively. Thus, outside of paddy areas, only the 8-day seasonal changes in LAI and FPAR were considered, and their yearly changes in each period were not considered.

One of the challenges in simulating rainfed rice production is data scarcity with respect to the crop calendar. Because rice is rainfed, the planting date is not fixed to a certain calendar date, and data on basin-wide planting dates are not available. We thus applied a satellite-data-based estimation method (Tsujimoto et al., 2021) using the 16-day Enhanced Vegetation Index (EVI) (MOD13Q1 and MYD13Q1 v006 products) (USGS, 2020b, 2020c) from MODIS to estimate the planting dates and used those for the rice growth simulations by mizuha. This algorithm was originally developed by Tsujimoto et al. (2019) by using field observation data in the Pursat River basin by Hirooka et al. (2016). Since the MODIS EVI is only available after 2000, we used the estimated results in 2016 for both the past and future simulations, taking into consideration that the planting dates in 2016 are considered an average over the last 20 years (Tsujimoto et al., 2021).

2.4. Past and future climate

A simulation of the 20-year period from January 1981 to December 2000 was conducted to compare the results with those for future climates and to validate the model with observations and statistics. The years from 1981 to 2000 are referred to as the past period in this study. For future climate, the outputs from the GCMs contributing to CMIP5 were used as a reference. Two projection periods, the near future (2041–2060) and the far future (2081–2100), were considered in this study under the Representative Concentration Pathway (RCP) 2.6, RCP4.5, and RCP8.5 scenarios. The meteorological data in the past and future periods were interpolated into 500 m × 500 m mizuha simulation grids using the inverse distance weight (IDW) method and linearly interpolated to hourly.

2.4.1. Past data

The Japanese 55-year Reanalysis data (JRA-55) (Harada et al., 2016; Hou et al., 2014; Kobayashi et al., 2015) were referenced to describe the past climate. Variables in the two-dimensional diagnostic fields (fcst_surf and fcst_phy2m) were used as forcing data in mizuha, including air temperature and specific humidity at 2 m height, wind speed at 10 m height, total cloud coverage, downward longwave radiation, downward solar radiation, and surface air pressure. These variables are provided at an approximately 55 km horizontal resolution and are available every three hours. In each simulation grid of mizuha, the air temperature was adjusted by the lapse rate based on the difference between the JRA-55 level (2 m) and the grid elevation.

For rainfall amount in the past period, the observation-based dataset, Asian Precipitation – Highly Resolved Observational Data Integration Toward Evaluation of Water Resources (APHRODITE) (Yatagai et al., 2012), was used. Its spatial resolution is 0.25° latitude by 0.25° longitude. Although the number of rain-gage stations in Cambodia is limited in the APHRODITE dataset, we compared the APHRODITE data for the past period with intensive rain-gage observation results from 2010 to 2015. The 20-year mean annual rainfall in 1981–2000 over the target basin was 1134 mm, which was comparable to the annual totals of 1087 to 1528 mm over Cambodia from 2010 to 2015 (Tsujimoto et al., 2018).

2.4.2. Evaluation and selection of GCMs

The acquisition, evaluation, and bias correction of the GCMs were performed using a tool for CMIP5 from the Data Integration and Analysis System (DIAS, https://diasjp.net) (Kawasaki et al., 2017). Among the 34 CMIP5 GCMs, we evaluated the 18 GCMs for which future projection data under RCP2.6, RCP4.5, and RCP8.5 were available at DIAS. The GCMs were evaluated from the viewpoint of rainfall reproductivity to be properly used for assessing rain-fed rice production.

For each GCM, the 20-year mean monthly rainfall during 1981–2000 were compared against data from the Global Precipitation Climatology Project (GPCP) (Adler et al., 2003) in the same period. The spatial correlation coefficient (SCORR) and root mean square error (RMSE) between the GCM and GPCP monthly rainfall were calculated by the following equations:

$$SCORR = \frac{\sum_{i=1}^{N}(x_i - \bar{x})(y_i - \bar{y})}{\sqrt{\sum_{i=1}^{N}(x_i - \bar{x})^2 (y_i - \bar{y})^2}} \tag{8}$$

$$RMSE = \sqrt{\frac{1}{N}\sum_{i=1}^{N}(x_i - y_i)^2} \tag{9}$$

where x_i and y_i are the GCM and GPCP rainfall at grid i, respectively, and $\bar{x}$ and $\bar{y}$ are the means of the GCM and GPCP rainfall over the entire grid in the study area, respectively. If SCORR = 1 for the spatial distribution and RMSE = 0 for the absolute value, then the spatial distribution pattern of the GCM outputs completely matches that of the GPCP.

To use both the SCORR and RMSE for GCM evaluation, the simple demerit point system used in Eastham et al. (2008) was adopted. In this study, the GCM performance was deemed poor when SCORR < 0.6 or RMSE > 2, and 1 demerit point was assigned to the GCM for each of the SCORR and RMSE indices that indicated poor performance. While Eastham et al. (2008) calculated the demerit points for rainy and dry seasons, we calculated them for each month to examine the rainfall reproducibility at fine temporal resolution. Thus, the maximum number of demerit points is 24 (2 indices × 12 months), where more demerit points correspond to lower reproducibility. In addition, to evaluate rainfall reproducibility for both monsoonal and local rainfall, we calculated demerit points over two regions, the Indochina Peninsula and Cambodia (domains 1 and 2, respectively; Fig. 2a), and summed their demerit points to select the best GCMs for assessing the impact of climate

change on rainfed paddy rice production in this region.

Since the calculated SCORR and RMSE showed a smaller difference among ensemble runs from each GCM compared with those among GCMs, we used only one ensemble member, r1i1p1, to calculate demerit points for all of the GCMs to maintain equitability regardless of the number of ensemble members of each GCM.

2.4.3. Bias correction of the GCM rainfall

Statistical bias correction was applied to the daily rainfall amounts in the selected GCMs. The details of this bias correction method are provided in Nyunt et al. (2016). In short, this method addressed the three main GCM deficiencies, i.e., underestimation of extremes, high frequency of rainy days, and poor seasonal simulation, through a 3-step statistical bias correction. Here, the GCM biases in the past climate were assumed to be stationary in the future climate, and the same transfer function ($F_{\mathrm{GCM_{past}}}$) derived from the GCM hindcast was applied to the GCM future projection:

$$x_{\mathrm{GCM_{past}}}{}' = {F_{\mathrm{obs}}}^{-1}\left(F_{\mathrm{GCM_{past}}}\left(x_{\mathrm{GCM_{past}}}\right)\right) \tag{10}$$

$$x_{\mathrm{GCM_{future}}}{}' = {F_{\mathrm{obs}}}^{-1}\left(F_{\mathrm{GCM_{past}}}\left(x_{\mathrm{GCM_{\mathit{future}}}}\right)\right) \tag{11}$$

where $x_{\mathrm{GCM_{past}}}{}'$ and $x_{\mathrm{GCM_{future}}}{}'$ represent bias-corrected GCM rainfall for past and future periods, respectively, and F_{obs} is the distribution function of the observed rainfall during the past period. The generalized Pareto distribution function was used in Eqs. (10)–(11) to determine $F_{\mathrm{GCM_{past}}}$ and F_{obs} to correct for extreme rainfall. The frequency of rainy days was then corrected by assuming the same number of rainy days in the observation as in the GCM hindcast. Using a simple rank-order statistic, the GCM rainfall corresponding to the same rank as that of the observation was defined as a correction threshold, and GCM future rainfall beyond this threshold was corrected to zero. Finally, monthly grouped normal rainfall was adjusted to fit a gamma distribution by mapping the cumulative distribution function of daily GCM rainfall to that of the observed rainfall, and corrections were made through Eqs. (10)–(11). In this study, APHRODITE was used as the observational data.

Through the bias correction process, rainfall from all the GCMs was spatially interpolated to the same grids as the reference, APHRODITE, which is 0.25° latitude by 0.25° longitude, although the original grid resolutions were different among the GCMs.

Only rainfall was bias corrected, and other meteorological variables (air temperature and humidity, wind speed, pressure, total cloud fraction, solar radiation, and longwave radiation at the ground surface) were used without bias correction. Data on radiation and cloud fraction for CCSM4 and CESM1(CAM5) were not available at DIAS and thus the equivalent data from MIROC5 were used for mizuha simulations with CCSM4 and CESM1(CAM5).

3. Results

3.1. Model validation

Because of the limited availability of basin-wide soil moisture data, river discharge was used for model validation on the spatiotemporal distribution of the simulated soil moisture, regarding river discharge as the spatially and temporally integrated result of soil moisture distribution in the basin. The availability of river discharge data (Masumoto et al., 2016) was limited to 2010–2011, and thus, the model parameters were calibrated against these two years. The comparison of observed and simulated river discharge is shown in Fig. 3. Although their agreement was not perfect, we adopted the calibrated parameters for the past and future simulations in this study because of the limited availability and uncertainties in both rainfall and river discharge data.

Since rice production statistics in the target basin were not available, the basin-averaged simulated results were compared with the nationwide FAO statistics (FAO, 2019) for yield, harvested area, and total production, as indicated in Fig. 4a–c. In these figures, yield (Fig. 4a) is shown as rice production (Fig. 4c) per unit harvested area (Fig. 4b). Changes in the harvested area occur both from changes in the sowed/planted area and from crop loss or damage over the entire sowed/planted area during cultivation. Clearly, increasing trends from the past to the present were recognized in yield and harvested area. These were considered to arise because of technological developments, such as increased fertilizer application, improvement in rice cultivars, increased irrigation, and agricultural land development. To distill the year-to-year fluctuation caused by meteorological factors, we calculated the anomalies from the trend, assuming a linear trend from 1981 to 2000. The anomalies in the FAO statistics showed correspondence with the simulation results by mizuha, especially in harvested area and total production, with lower production in 1984, 1987, and 1994 and higher production in 1989, 1995, and 1999. Fig. 4d shows the scatter plot between the anomalies of production in the FAO statistics and the mizuha simulation, indicating that the overall characteristics of year-to-year fluctuation were well described by mizuha, although they are not in perfect agreement. In this study, we used this model and these parameters for past and future simulations.

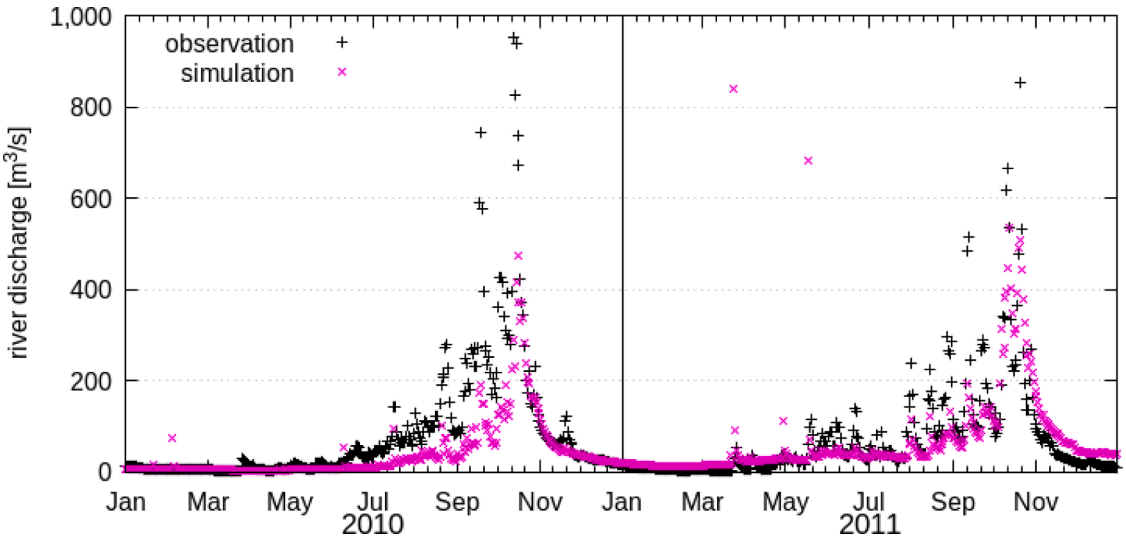

Fig. 3. Observed and simulated river discharge in the Pursat River in 2010–2011. The observed river discharge data are from Masumoto et al. (2016).

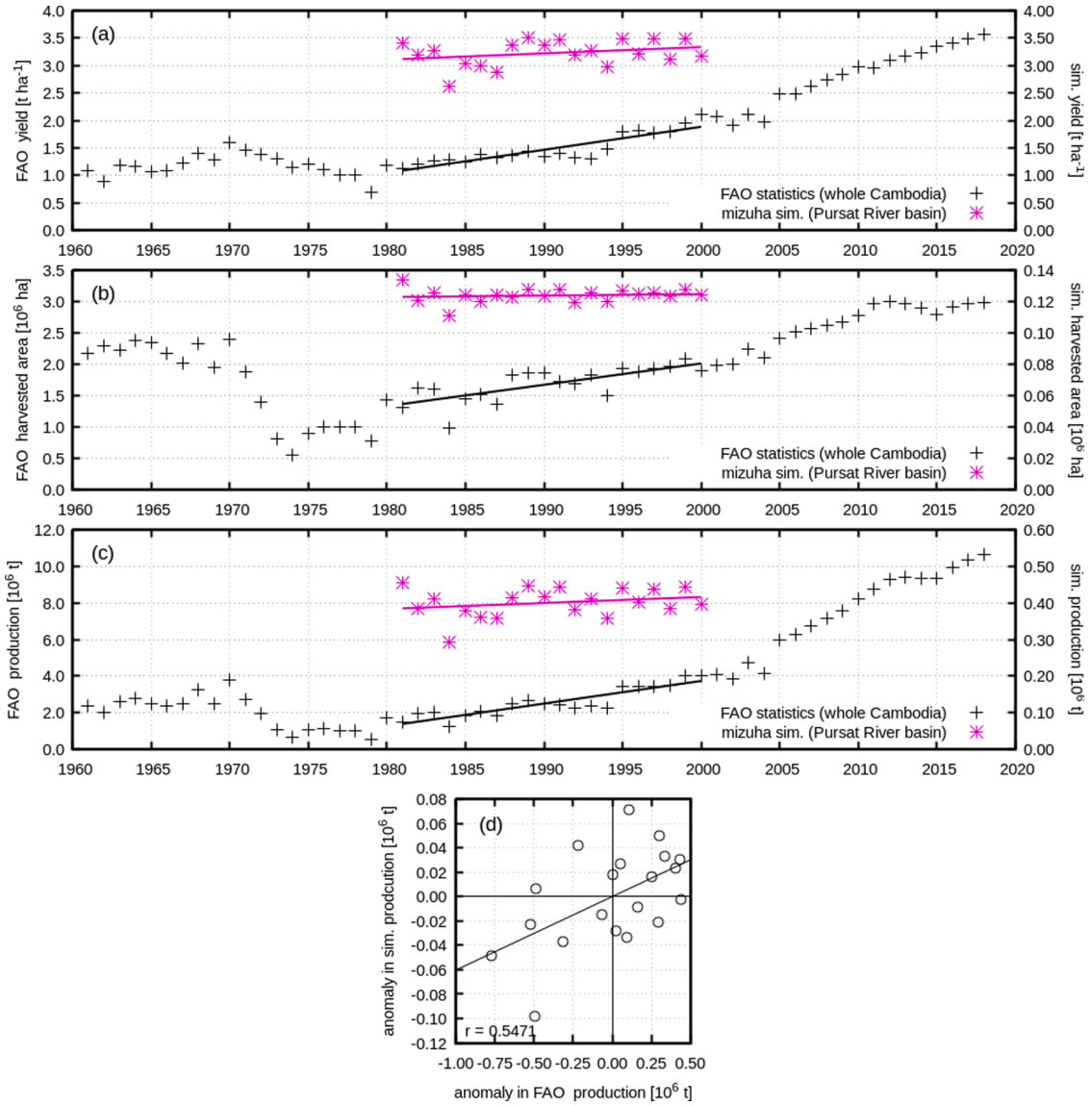

Fig. 4. Comparison of the FAO statistics (nationwide) and the simulated values (Pursat River basin) for (a) yield, (b) harvested area, and (c) total production of rice crops. The simulated values are indicated on the right axes. The period from 1981 to 2000 is the simulation period for the past run in this study. Yield in (a) is the value over the harvested area only (totally damaged paddies that were planted but not harvested were not included to calculate yield). (d) Scatterplot between the anomalies of production from trends in FAO statistics and simulation.

3.2. Past and future rainfall by the selected GCMs

The evaluation results of the 18 GCMs from CMIP5 are listed in Table 2. The five GCMs with the smallest demerit points were CCSM4, CESM1(CAM5), MIROC5, MPI-ESM-LR, and NorESM1-M, as shown with asterisks in Table 2. As explained in the earlier section with Eqs. (8)–(9), the selected GCMs with smaller demerit points have relatively high SCORRs and low RMSEs for monthly rainfall reproducibility in the past through January to December, and thus it is generally recognizable that future rainfall predictions by these GCMs are more reliable than others both in their absolute values (from RMSEs) and spatial distributions (from SCORRs). Thus, we adopted these 5 GCMs in this study to assess rain-fed rice production for this region.

The daily rainfall amounts from these selected GCMs are shown in Fig. 5 along with the reference data from APHRODITE to show the validation of the reproducibility of the daily basis rainfall amount by the selected GCMs and the effectiveness of the bias correction applied in this study. The daily rainfall amounts on all the days in each month from May to December over the 20 years were plotted as jitter plots and boxplots for the past (1981–2000) and future (2041–2060 under RCP4.5) periods. Overall, all the selected GCMs were found to overestimate past rainfall compared with APHRODITE. After bias correction was applied, the medians and the other quartile values of the past rainfall estimates of the GCMs were comparable to those of APHRODITE, as shown in the boxplots. Using the same transfer function, future rainfall projections were corrected to be smaller than their original values in almost all the GCMs and months. These bias-correction results indicate that even through selecting the better-performing GCMs in representing the past rainfall, they tend to overestimate the future annual rainfall for this region; thus, they will underestimate the drought damage on rain-fed rice production if they are applied without bias correction.

Based on the bias-corrected future rainfall, the 20-year averaged annual total amount in 2041–2060 under RCP4.5 was 1190 mm (CCSM4), 1328 mm (CESM1(CAM5)), 1216 mm (MIROC5), 1227 mm (MPI-ESM-LR), and 1343 mm (NorESM1-M), showing a slight (5~18%) increase compared with the past period (1134 mm in APHRODITE). Thus, it is very likely that annual rainfall in Cambodia will increase in

Table 2
Evaluation results of the 18 GCMs from CMIP5 shown with the calculated demerit points. Fewer demerit points correspond to higher reproducibility, with the maximum number of demerit points set to 24 for each domain. The asterisks (*) by the GCM name indicate the five GCMs that were selected in this study.

GCM name	Country	Demerit points Domain 1 + 2	Domain 1: Indochina Peninsula	Domain 2: Cambodia
CCSM4*	USA	17	10	7
CESM1(CAM5)*	USA	24	14	10
MIROC5*	Japan	23	16	7
MPI-ESM-LR*	Germany	24	15	9
NorESM1-M*	Norway	24	13	11
BCC-CSM1.1	China	28	15	13
CanESM2	Canada	28	18	10
CNRM-CM5	France	27	17	10
CSIRO-Mk3.6.0	Australia	31	17	14
FGOALS-g2	China	32	17	15
GFDL-CM3	USA	28	14	14
GFDL-ESM2G	USA	31	17	14
IPSL-CM5A-LR	France	29	17	12
IPSL-CM5A-MR	France	26	17	9
MIROC-ESM	Japan	36	19	17
MIROC-ESM-CHEM	Japan	34	17	17
MPI-ESM-MR	Germany	28	16	12
MRI-CGCM3	Japan	29	16	13

the future.

From the viewpoint of agricultural water resources, however, not only annual total but also its seasonal distribution is important. Fig. 6 shows the bias-corrected future monthly rainfall compared with the past data in APHRODITE, shown as the areally averaged values for each subbasin (subbasin 9 for the upper stream and 1 for the lower stream, as their locations are shown in Fig. 2b). In Fig. 6, the rainy season in the past was approximately May–October, with rainfall peaking in September–October. In the future, the rainfall peak was projected to be earlier in CCSM4 and CESM1(CAM5), shifting to August–September with less rainfall in October. In MPI-ESM-LR, two rainfall peaks, in May–June and September, were projected. In MIROC5, the rainfall peak was projected to be later with increased rainfall in September–October and less rainfall in the early rainy season in June–July. The rainfall amount was larger in the upper subbasins (7–9) than in the lower subbasins (1–5) in the past, and the difference between the upper and lower subbasins tended to become more pronounced in the future in all the GCMs, especially in the months with abundant rainfall. The future rainfall tendency was recognized to be common regardless of the future periods and RCP scenarios (see Fig. S1 in the Supplementary Material).

3.3. Rice production

3.3.1. Projected change in rice production

The effects on rice production appeared as both damaged areas and yield losses. Fig. 7 shows simulated rice yield under the past and future (2041–2060) climates indicated with the percentages of the damaged (planted but not harvested) areas (see Fig. S2 in Supplementary Material for 2081–2100). The future simulations with CCSM4 and CESM1(CAM5) showed little change in yield regardless of the periods and RCP scenarios, whereas the results with MIROC5 and NorESM1-M showed remarkable decreases in future yield compared with the past run with APHRODITE. Especially in the simulation with MIROC5 for 2041–2060 under the RCP4.5 scenario, frequent occurrences of low yield at less than 250 t ha^{-1} were projected. In simulations with NorESM1-M, not only the median but also the maximum yields were projected to decrease under all three RCP scenarios in the near and far future periods, with little difference among scenarios/periods. The differences among scenarios/periods were larger in MIROC5 and MPI-ESM-LR than in the other models, and these two models showed larger year-to-year and location-to-location fluctuations (indicated by longer boxplots).

The totally damaged area was 11.3% in the past run, and the ratio was similar or even smaller in the future runs with CCSM4 (9.9~10.8%), CESM1(CAM5) (9.7~10.5%), and NorESM1-M (9.9~10.6%) regardless of the periods or RCP scenarios. However, in future runs with MIROC5 (13.0~18.7%) and MPI-ESM-LR (14.5~16.3%), increases in the totally damaged area were projected.

3.3.2. Affecting factors on rain-fed rice production

Under the given conditions in this study, i.e., nonirrigated rainfed paddies with constant CO_2 concentrations and fertilizer application rates, fixed rice cultivars, and without consideration of pests and diseases, water stress to rice plants is the most important potential factor for lower rice production. Fig. 8 shows the root-zone soil moisture in the rice growing season. In the results from MIROC5, in which simulated rice production was lower than that of the other GCMs, soil moisture was comparable to that of the past and future simulations with the other GCMs at the beginning (May) and end (October) of the rainy season, but it was lower in the early rainy season in June and July. In addition, the soil moisture variability was larger in July and August, with the frequent occurrence of distinctively low soil moisture. Such dry spells just after the beginning of the rainy season in July are often observed in Cambodia, causing serious damage to agriculture. More severe dry spells were projected in MIROC5 than in the other GCMs during the early rainy season over this region. Similarly, in the simulations with MPI-ESM-LR, which showed high variability in rice production as with MIROC5 in Fig. 7, large fluctuations in soil-water availability throughout the rainy season under future climates are projected. On the other hand, in the simulated results from CCSM4 and CESM1(CAM5), in which simulated rice production was larger than that of the other GCMs, the median simulated soil moisture was higher than that of the past with relatively small variability in all rainy-season months.

The simulation results with NorESM1-M are unique in that it showed lower production than that of the other GCMs (Fig. 7), while its soil moisture was similar to that of the high-yield simulations with CCSM4 and CESM1(CAM5) (Fig. 8). This suggests the existence of other factors affecting rice production under climate change. Fig. 9 shows the other meteorological forcing data used to run mizuha for the past and future periods. Fig. 9 reveals that NorESM1-M projected less shortwave radiation and a higher cloud fraction during the rainy season, from May to November, than those of the other GCMs and JRA-55. Thus, the air temperature was lower in NorESM1-M than in the other GCMs and even in the past reanalysis of JRA-55, even though the projections with climate change are under increased radiative forcing. The projected low solar radiation and air temperature are considered to be the reasons why rice production was consistently lower in simulations by mizuha with

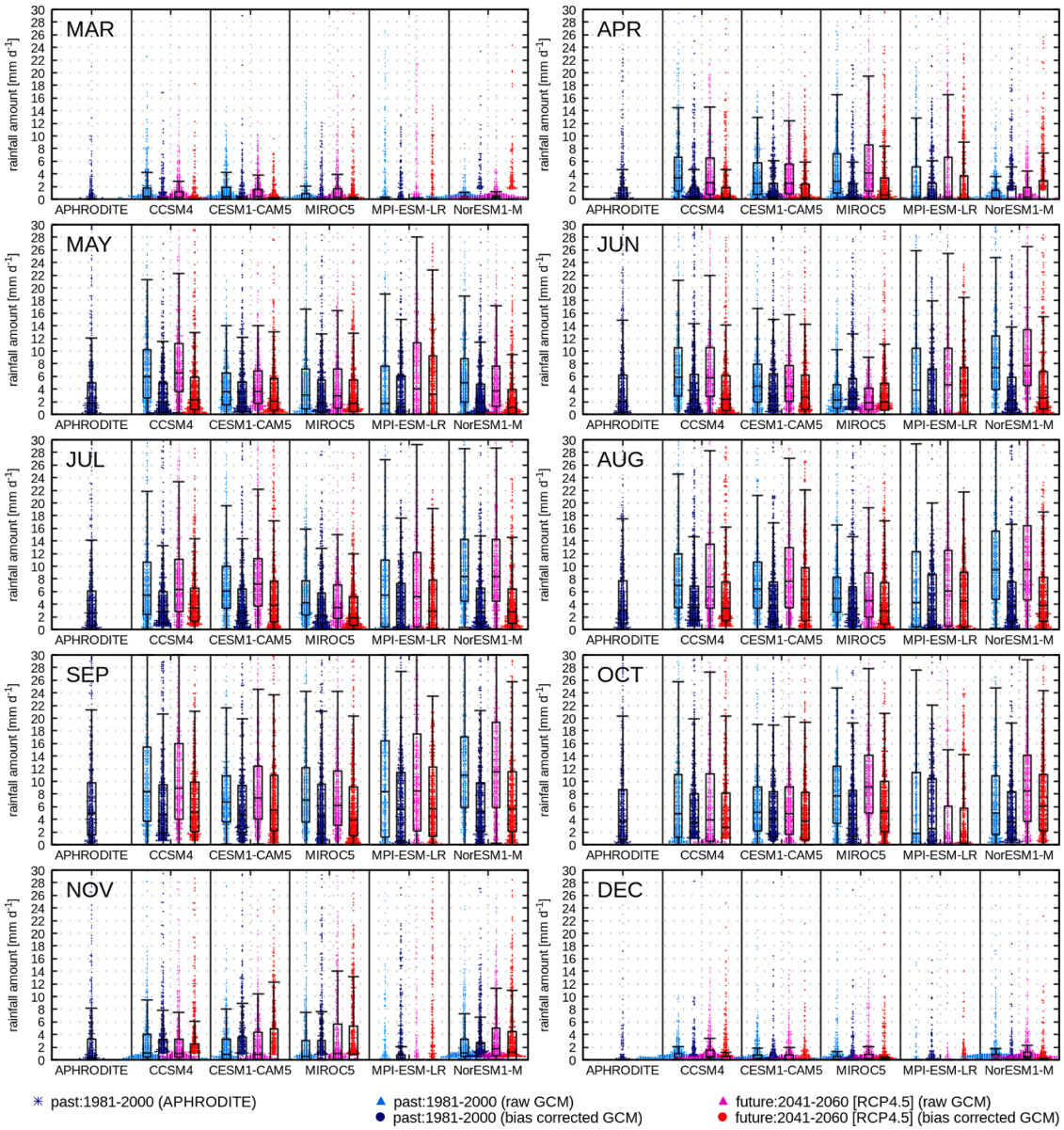

Fig. 5. Daily rainfall in March–December from APHRODITE (1981–2000) and the five selected GCMs (CCSM4, CESM1(CAM5), MIROC5, MPI-ESM-LR, NorESM1-M). For GCMs, outputs for the past (1981–2000) and future (2041–2060, RCP4.5) periods are shown with and without bias corrections. The number of data points is 20 × (the number of days in the month) for each jitter plot and boxplot (minimum, lower quartile, median, upper quartile, and maximum values without outliers are shown). All the data are over the study area at 12.5° N, 104.0° E.

NorESM1-M than the other GCMs.

This result highlights the importance of the solar radiation amount during the rainy season or the relationship between rainfall and solar radiation. This relationship is closely linked with the diurnal cycle of rainfall or convective activity because if rainfall and cloud coverage are concentrated at night, the amount of daily solar radiation does not decrease even on rainy days. In earlier studies, the diurnal and seasonal distributions of solar radiation in Cambodia were observed to be as strong in the rainy season as in the dry season because of the predominantly evening rainfall (Tsujimoto et al., 2008, 2018) and convective activity from midnight to early morning over Tonle Sap Lake and its lakeshore (Tsujimoto et al., 2018). As Tsujimoto et al. (2008) pointed out, the diurnal cycle of rainfall and the amount of solar radiation on rainy days differ across regions and seasons, and thus, it is important to take them into consideration when assessing the factors affecting agricultural production in the region. This study suggests the importance of considering the reproducibility of the diurnal cycle of rainfall, convective activity, and solar radiation to assess the impact of climate change on crop production, which depends on solar radiation, air temperature, and rainfall.

4. Discussion

4.1. Future projection of rice production in Cambodia

The assessment of climate change impacts in data-scarce regions was one of the major challenges in this study, especially in conducting assessments not only at the field scale but also at the basin scale considering the basin hydrological cycle and spatial distribution of rainfall and soil moisture within a basin. Although uncertainty remains, the following five points are suggested from this study.

First, excluding NorESM1-M, two out of four GCMs (CCSM4 and CESM1(CAM5)) showed little change in future rice production compared with that of the past in terms of the median and other quartile

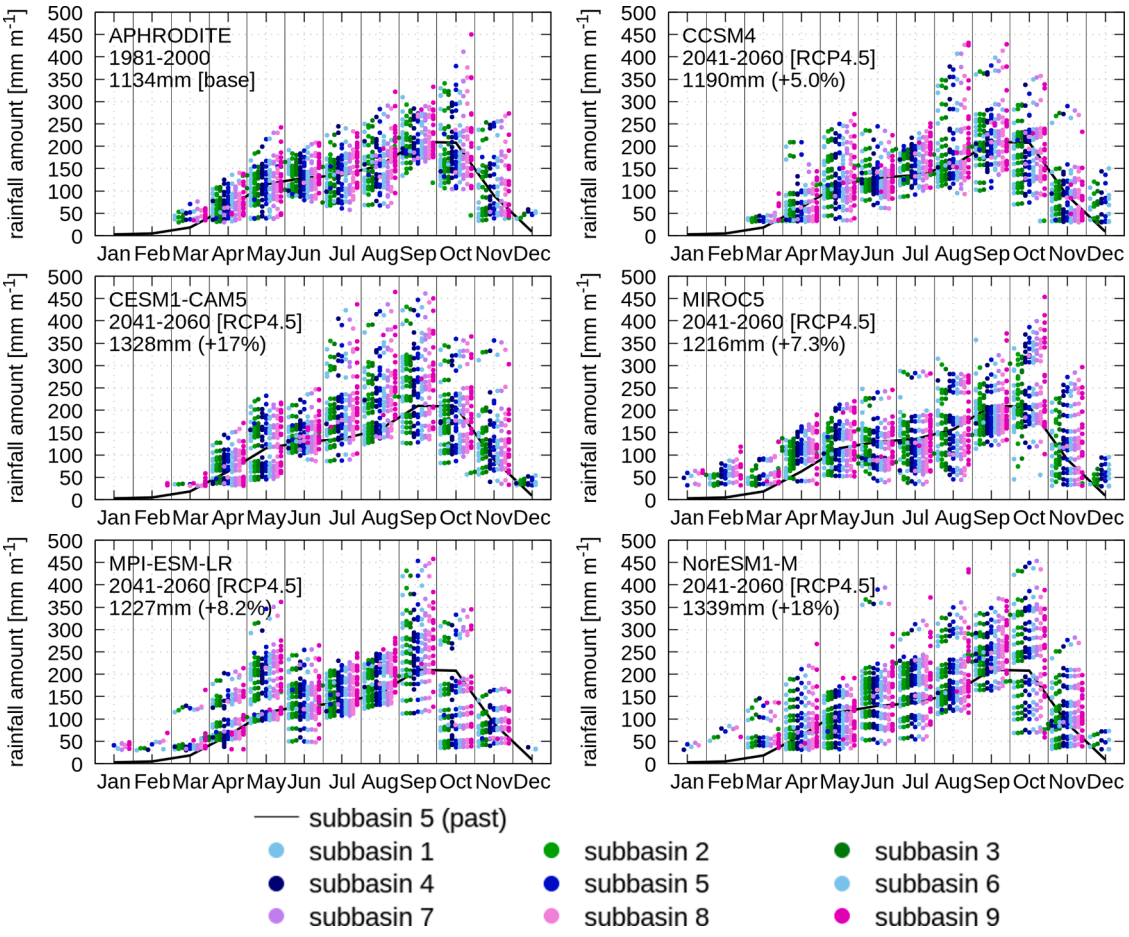

Fig. 6. Monthly rainfall in the five GCM future projections compared with past observations (APHRODITE). Spatially interpolated rainfall as areal averages for subbasins 1–9 (see Fig. 2b for their locations) are shown. Past data for subbasin 5 are shown with a black line in each panel for reference. The annual total rainfall and its change ratio against APHRODITE at 12.5° N, 104.0° E are indicated in the top left of each panel. See Fig. S1 in the Supplementary Materials for the other future period and RCP scenarios.

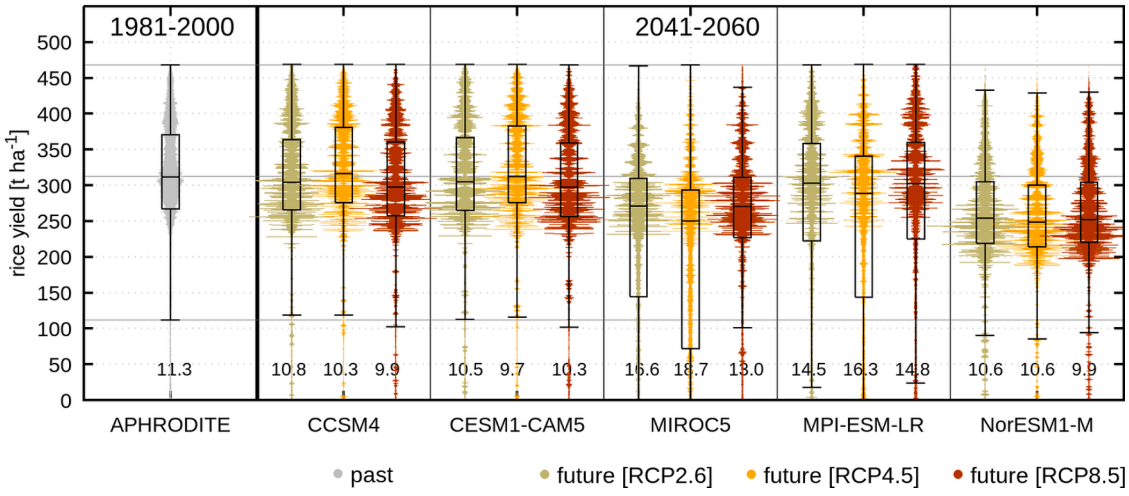

Fig. 7. Simulated rice yield under the past and future climate conditions in 2041–2060 under the RCP2.6, 4.5, and 8.5 scenarios. The data in each plot are from all the paddy grids (5585 grids) over 20 years (111,700 points), shown as jitter plots and boxplots (the minimum, lower quartile, median, upper quartile, and maximum values without outliers are shown). Points with yield = 0 are not shown in the jitter plots to improve the visibility of the graph. At the bottom of each plot, the percentage of the number of paddy grids with yield = 0 (i.e., totally damaged area = planted area – harvested area) to the total planted area is indicated. See Fig. S2 in the Supplementary Material for 2081–2100.

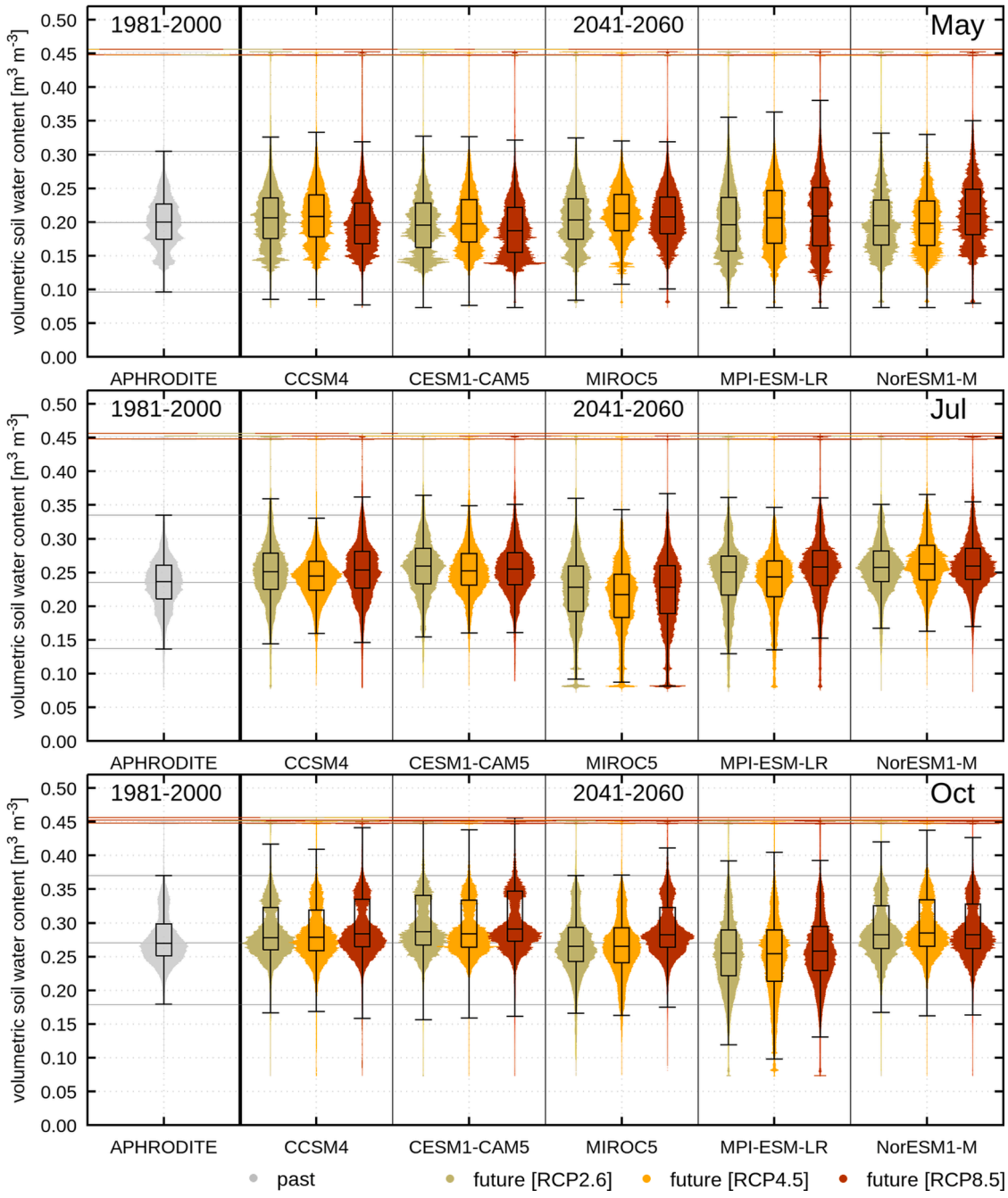

Fig. 8. Same as Fig. 7 but for the root-zone (top 50 cm) soil moisture (volumetric soil-water content in $m^3\ m^{-3}$) in May, Jul, and October. Data at 2:00 LT and 14:00 LT each day are taken for each plot; the number of data points in each plot is 5585 paddy grids × 20 years × 365 days × 2 times/day = 81,541,000. See Fig. S3 in the Supplementary Material for other months and future periods.

values from basin-wide statistics over 20 years. However, the year-to-year and location-to-location fluctuations (shown as the width of the jitter plots) in the future are much larger than those in the past, even in the simulations with CCSM4 and CESM1(CAM5). This suggests higher spatiotemporal variability in rice production in the basin, which can be a great threat to individual farmers even though rice production on a basin scale may not be significantly impacted. Under such conditions, a framework to share or allocate potential risks and resources within the basin may be an effective long-term risk management strategy.

Second, considering that one of the selected GCMs (MIROC5) suggested the potential intensification of dry spells in the early rainy season, preparation for supplementary irrigation in this season or a shifting of the crop calendar may be options as adaptation strategies.

Third, since most of the selected GCMs showed an increase in the regional difference in rainfall between the upper and lower basins in the Pursat River basin, with more rainfall in the upper basin and less rainfall in the lower basin where most of the paddies are located, the effective storage of excess rainfall from the upper basin using reservoirs, along with irrigation facilities in downstream paddy fields, can also be an option.

Fourth, differences among the future periods (either the near future in 2041–2060 or far future in 2081–2100) and RCP scenarios (RCP2.6, RCP4.5, RCP8.5) were not significant in the simulations with CCSM4, CESM1(CAM5), and NorESM1-M, whereas they were large in MIROC5 and MPI-ESM-LR. From this study, it is difficult to conclude whether the impact on rice production changes with time or with RCP. Rather,

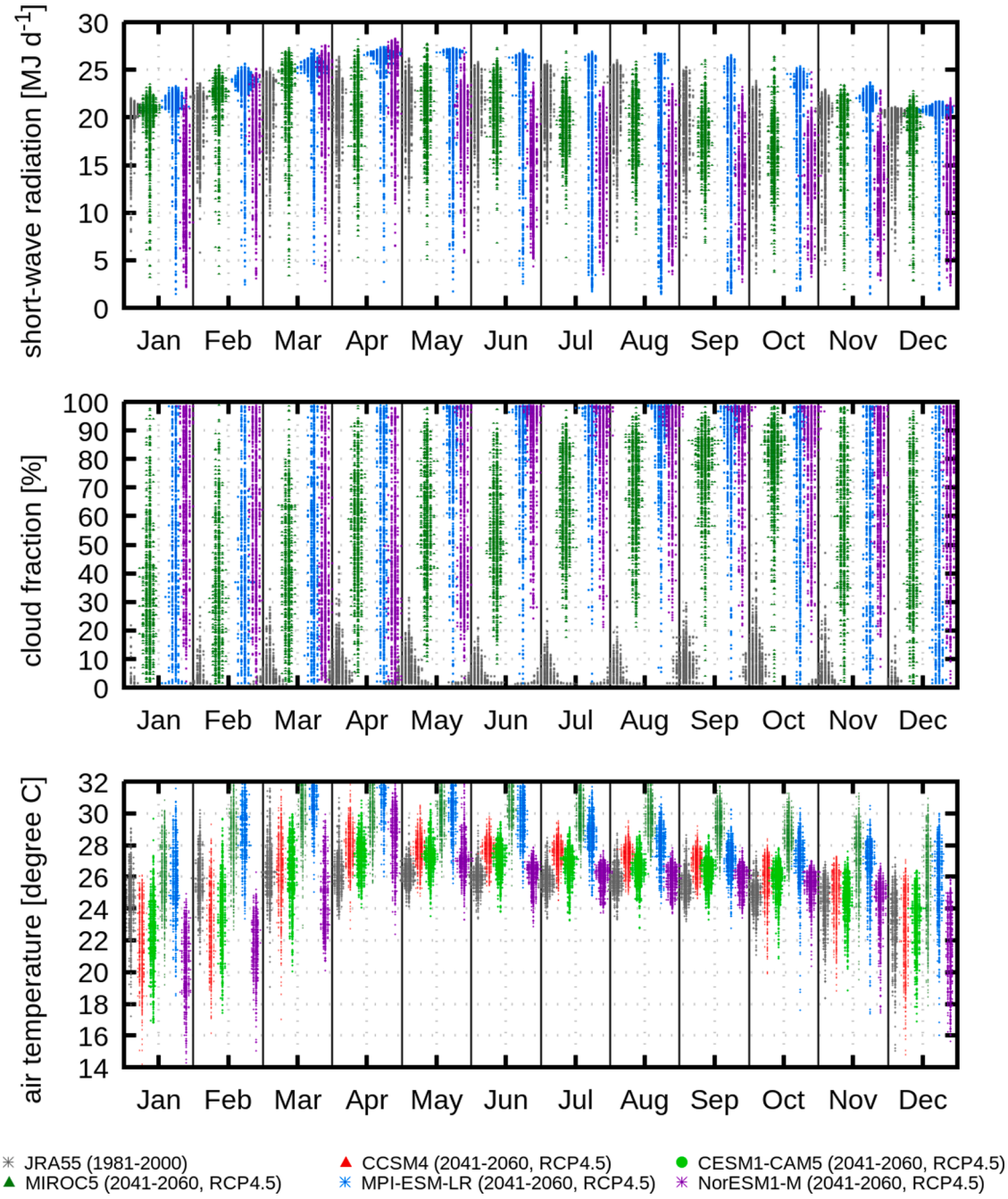

Fig. 9. Meteorological forcing data from the JRA-55 reanalysis (1981–2000) and GCM future projections (2041–2060, RCP4.5). Daily data for 20 years in each month are shown for locations at 12.5° N, 104.0° E. Radiation and cloud fraction data were not available at the DIAS for CCSM4 and CESM1(CAM5).

further investigation of the rainfall pattern that affects rainfed paddy rice production should be taken to improve the methods for climate change impact assessment of rice production, including the improvement, selection, and bias correction of GCMs.

Finally, although this study neglected the effects of increasing CO_2 concentrations, rice yield has been reported to increase with more CO_2. In addition, the effects of the changes in CO_2 as well as soil moisture, solar radiation, and air temperature differ among different rice cultivars. Changes in the application rate of fertilizer and irrigation clearly affect rice production, but the extent of their effects also depends on the cultivar (Iwahashi et al., 2021; Kodo et al., 2021). Moreover, as such changes in agronomic management, shifts in the crop calendar, especially on planting dates, are known to affect rice production even under the same meteorological conditions (Hirooka et al., 2016). Using the present study as a base scenario, effective adaptation strategies that also consider other effects, such as cultivars, CO_2 concentration, fertilizer, irrigation, and crop calendar, should be examined.

4.2. Quantification of the GCM-related uncertainties and suggestions from the viewpoint of GCM application to rain-fed rice production simulations

In an earlier study that examined changes in soil moisture under climate change, Saseendran et al. (2000) assessed the tropical humid climate in India and suggested that increased rainfall will increase soil moisture and thus increase rice production. Similarly, Sun et al. (2019) projected future agricultural drought in the Yangtze River basin in China under climate change and suggested an increase in soil moisture.

However, these studies examined changes in rainfall and soil moisture on an annual or monthly basis without considering finer temporal scale distributions or the duration of dry spells. Our study showed the importance of analysis with a higher temporal resolution than annual or monthly to assess the impact of soil moisture on rice production, as dry spells lasting less than 1 month can severely affect rice growth, and thus monthly or annually based evaluation can underestimate the drought damage to rice production. This is especially the case for Cambodia, where the annual rainfall is projected to increase.

To properly take into consideration the effect of soil moisture deficiency on rain-fed rice production, the methodologies for the selection and bias correction of the GCMs as well as for downscaling simulation of the soil-water flow in the basin are the key to improving the accuracy of future projections. These are the keys of this study. In a similar study over the Lower Mekong River basin, Ruan et al. (2018) ranked the 34 GCMs in CMIP5 according to their rainfall reproducibility against the APHRODITE data using RMSE, SCORR, and six other statistical indices. MPI-ESM-LR was selected as the best model, followed by IPSL-CM5A-MR, when the GCMs were evaluated by their rainy season (May–October), dry season (November–April), and annual total rainfall accumulations. The scores for CCSM4 and CESM1(CAM5) were also high, with better scores for the dry season in CCSM4 and for the rainy season in CESM1(CAM5). The other two GCMs selected in our study, NorESM1-M and MIROC5, were ranked 12th and 20th, respectively. However, in evaluating rainfall reproducibility over the Mekong River basin at monsoon onset with the GPCP and other data, Hasson et al. (2016) found a better performance in CCSM4, MIROC5, and NorESM1-M than in CESM1(CAM5) and MPI-ESM-LR. Comparing the results of our study with these earlier studies, we can see that the evaluation of GCMs is highly dependent on the evaluation periods and metrics. This suggests the importance of examining the appropriate time span when evaluating GCMs for assessing impacts on rice production. Considering the potential time span that is critical for rainfed rice, a shorter period rather than annual or seasonal periods will be more effective for evaluating rainfall reproducibility. In this regard, the GCMs that were selected in this study based on monthly rainfall were considered more suitable than those selected in earlier studies for assessing the impact of climate change on rainfed rice production.

The predictability of dry spells during monsoonal rainfall was suggested to be important because farmers generally start planting rainfed paddies in accordance with the onset of the rainy season. Since rainfall or soil-water availability during the early growing season is important for successful rice growth, the predictability of dry spells greatly affects the accuracy of rainfed paddy rice production estimates. Although the escalating number of dry spells in the early monsoon season was projected only by MIROC5 and not by the other four GCMs, Hasson et al. (2016) found that MIROC5 had a better performance in reproducing rainfall at the monsoon onset. This suggests that detailed examination of the reproducibility and future projection of rainfall at monsoon onset and of dry spells is required.

In addition, this study indicates the potential overestimation of daily rainfall amount by the GCMs throughout the rainy season for this region - even for the selected GCMs - and suggests the importance of bias correction, in addition to the selection, of the GCMs. However, the bias correction method also needs to be examined further. In the bias correction method used in this study, GCM biases were considered to be stationary from the past to the future, and the same transfer function was applied for the GCM hindcasts and predictions. The weak rainfall features in GCMs that were under a determined threshold value derived from the hindcast were then removed completely. As a result, in the bias-corrected GCM outputs, weak rainfall was artificially removed in some months and models: this is apparent in Fig. 5 for March and April in NorESM1-M, for June in MIROC5, from July through November in CCSM4, and for October–November in CESM1(CAM5). However, because even weak rainfall can have an important effect on the wetness of the root-zone soil, accurate bias correction of rainfall to reproduce root-zone soil wetness is necessary when using GCMs to assess the impact of climate change on agriculture. The removal of weak rainfall in MIROC5 in June is considered one reason for the decreased soil moisture in June and lowered rice production in the mizuha simulations with MIROC5. Although this study directly applies the bias correction method by Nyunt et al. (2016), the bias correction method itself should be further examined depending on the objectives to use future rainfall data, and for assessing rain-fed rice production, the bias correction method for weak rainfall events should be improved.

Finally, the reproducibility of solar radiation in connection with the diurnal cycle of rainfall was also shown to be important for NorESM1-M. Although atmospheric processes are calculated at a finer time resolution than daily, for the application of GCM outputs to climate change impact assessments of agriculture and other socioeconomic sectors, often only daily or monthly data are used, and GCM evaluation is also conducted at these time scales. This study showed the importance of evaluating GCM rainfall with its diurnal cycle to select GCMs that have higher reproducibility not only for rainfall but also for radiation and air temperature, which are the three important limiting factors for crop production. The simulated results with NorESM1-M in this study were thus not considered reliable because of the observed relationship between rainfall and solar radiation. However, changes in the diurnal cycle of rainfall and its effect on solar radiation on rainy days may also change in the future. This aspect should be monitored when assessing the agricultural impacts of climate change.

5. Conclusions

Through the evaluation and bias correction of the GCMs that participated in CMIP5, all five selected GCMs showed future increases in annual rainfall in this region under all three RCP scenarios. Despite the commonly projected increase in rainfall on an annual basis, the projected effect on rain-fed rice production differed depending on the GCMs to force the rice model, and three out of five selected GCMs resulted in a projected decrease in rice production. The major cause was revealed to be the changes in the seasonal distribution of rainfall, and it was different among the five GCMs. The rainfall peak was projected to shift earlier in CCSM4 and CESM1(CAM5) to August–September with less rainfall in October; two rainfall peaks, in May–June and September, were projected in MPI-ESM-LR; and in MIROC5, the rainfall peak was projected to shift later with increased rainfall in September–October and less rainfall in June–July.

The simulated lower yield with NorESM1-M was attributable to the projected lower solar radiation, which was considered erroneous based on the observed solar radiation. For simulations with MIROC5 and MPI-ESM-LR, high variability in lower-than-average root-zone soil moisture was considered the main factor restricting rice production. In MIROC5, dry spells in the early monsoon season were projected to be more severe than those in the other GCMs. These results suggest the importance of the ability of GCMs to project the diurnal cycle of rainfall (or solar radiation on rainy days). They also show the importance of using accumulated rainfall amount in shorter periods than annual or seasonal (in the time scale of the potential damage to rice growth), including the onset and withdrawal of the monsoons, timing and length of dry spells, and weak rainfall events.

In using the present results for policy making, this study raises the importance of improving the projection ability of climate, which includes the improvement of GCMs themselves and of methods for their evaluation, selection and bias correction. The appropriate methods may differ depending on the objectives; for example, those for assessing the impact on agriculture may differ from those for assessing flood risk. The examination and establishment of appropriate methods for targeting the assessment of vegetation/crop growth are greatly needed, in addition to the continuous improvement of the predictability of atmospheric fields by global and regional climate models.

For reliable future projections, in addition to model development,

access to local data on related variables and human-related activities such as land-use distribution and agricultural management (crop calendar, application of irrigation, fertilizer, pesticide application, and so on) are essential for the calibration, validation, and bias correction of the models. Such hydrometeorological and agricultural data, especially those in long-term periods, in turn will contribute to future projection accuracy and to promoting the socioeconomic development of the country and thus will be highly encouraged.

CRediT authorship contribution statement

K. Tsujimoto: Conceptualization, Methodology, Software, Validation, Formal analysis, Investigation, Visualization, Writing – original draft, Writing – review & editing. **N. Kuriya:** Formal analysis, Investigation, Writing – original draft. **T. Ohta:** Methodology, Software, Formal analysis, Investigation, Visualization, Writing – review & editing. **K. Homma:** Methodology, Software, Validation, Formal analysis, Investigation, Writing – review & editing. **M.So Im:** Conceptualization, Validation, Investigation, Writing – review & editing.

Declaration of Competing Interest

The authors declare that they have no known competing financial interests or personal relationships that could have appeared to influence the work reported in this paper.

Acknowledgements

We are deeply grateful to Prof. Emeritus Toshio Koike of the University of Tokyo for the long-term support and valuable comments. We thank Prof. Takao Masumoto of Akita Prefectural University for providing river discharge data in the Pursat River basin. We greatly appreciate the kind support from H.E. Mr. Pich Veasna, H.E. Mr. Long Saravuth, Mr. Mao Hak, Mr. Oum Ryna, and Mr. Yoshihiro Doi of the Ministry of Water Resources and Meteorology, Cambodia, for facilitation of the study in Cambodia. The CMIP5 datasets for this research were obtained from and are available from the DIAS website (https://diasjp.net/). We are grateful to the Editor-in-Chief Dr. Juan A. Blanco and three anonymous reviewers for their helpful and constructive comments that greatly contributed to improving the manuscript from the earlier version.

Funding

Parts of this research were supported by the Japan Society for the Promotion of Science (JSPS) KAKENHI Grant Numbers JP16K06503 and JP19KK0171, by the IDEA Consultants, Inc. Research Project, and by the Earth Observation Collaborative Research (PI Number ER2GWF101) and Precipitation Measuring Mission (PMM) 7th Research Announcement projects by JAXA.

Supplementary materials

Supplementary material associated with this article can be found, in the online version, at doi:10.1016/j.ecolmodel.2021.109815.

References

Adler, R.F., Huffman, G.J., Chang, A., Ferraro, R., Xie, P.P., Janowiak, J., Rudolf, B., Schneider, U., Curtis, S., Bolvin, D., Gruber, A., Susskind, J., Arkin, P., Nelkin, E., 2003. The version-2 global precipitation climatology project (GPCP) monthly precipitation analysis (1979–Present). J. Hydrometeorol. 4, 1147–1167 https://doi.org/10.1175/1525-7541(2003)004<1147:tvgpcp>2.0.co;2.

Ainsworth, E.A., Long, S.P., 2005. What have we learned from 15 years of free-air CO2 enrichment (FACE)? A meta-analytic review of the responses of photosynthesis, canopy properties and plant production to rising CO2. New Phytol. 165, 351–372. https://doi.org/10.1111/j.1469-8137.2004.01224.x.

Arunrat, N., Pumijumnong, N., Hatano, R., 2018. Predicting local-scale impact of climate change on rice yield and soil organic carbon sequestration: a case study in Roi Et Province, Northeast Thailand. Agric. Syst. 164, 58–70. https://doi.org/10.1016/j.agsy.2018.04.001.

Babel, M.S., Agarwal, A., Swain, D.K., Herath, S., 2011. Evaluation of climate change impacts and adaptation measures for rice cultivation in Northeast Thailand. Clim. Res. 46, 137–146. https://doi.org/10.3354/cr00978.

Boonwichai, S., Shrestha, S., Babel, M.S., Weesakul, S., Datta, A., 2019. Evaluation of climate change impacts and adaptation strategies on rainfed rice production in Songkhram River Basin. Thailand. Sci. Total Environ. 652, 189–201. https://doi.org/10.1016/j.scitotenv.2018.10.201.

Bouman, B., Tuong, T., Kropff, M., van Laar, H., 2001. The model ORYZA2000 to simulate growth and development of lowland rice. In: Ghassemi, F., White, D., Cuddy, S., Nakanski, T. (Eds.), MODSIM 2001, Integrating Models for Natural Resources Management Across Disciplines, Issues and Scales: International Congress on Modelling and Simulation, Canberra 2001. The Modelling and Simulation Society of Australia and New Zealand Inc., Canberra, pp. 1793–1798.

Darzi-Naftchali, A., Karandish, F., 2019. Adapting rice production to climate change for sustainable blue water consumption: an economic and virtual water analysis. Theor. Appl. Climatol. 135, 1–12. https://doi.org/10.1007/s00704-017-2355-7.

Deb, P., Tran, D.A., Udmale, P.D., 2016. Assessment of the impacts of climate change and brackish irrigation water on rice productivity and evaluation of adaptation measures in Ca Mau province. Vietnam. Theor. Appl. Climatol. 125, 641–656. https://doi.org/10.1007/s00704-015-1525-8.

Eastham, J., Mpelasoka, F., Mainuddin, M., Ticehurst, C., Dyce, P., Hodgson, G., Ali, R., Kirby, M., 2008. Mekong River Basin Water Resources Assessment: Impacts of Climate Change. CSIRO, Canberra, Australia.

FAO, 2007. FAO Digital Soil Map of the World. (DSMW). FAO, Rome, Italy.

FAO, 2019. FAOSTAT. FAO, Rome, Italy.

Harada, Y., Kamahori, H., Kobayashi, C., Endo, H., Kobayashi, S., Ota, Y., Onoda, H., Onogi, K., Miyaoka, K., Takahashi, K., 2016. The JRA-55 reanalysis: representation of atmospheric circulation and climate variability. J. Meteorol. Soc. Jpn. II 94, 269–302. https://doi.org/10.2151/jmsj.2016-015.

Hasson, S., Pascale, S., Lucarini, V., Böhner, J., 2016. Seasonal cycle of precipitation over major river basins in South and Southeast Asia: a review of the CMIP5 climate models data for present climate and future climate projections. Atmos. Res. 180, 42–63. https://doi.org/10.1016/j.atmosres.2016.05.008.

He, L., Cleverly, J., Wang, B., Jin, N., Mi, C., Liu, D.L., Yu, Q., 2018. Multi-model ensemble projections of future extreme heat stress on rice across southern China. Theor. Appl. Climatol. 133, 1107–1118. https://doi.org/10.1007/s00704-017-2240-4.

Hirooka, Y., Homma, K., Kodo, T., Shiraiwa, T., Soben, K., Chann, M., Tsujimoto, K., Tamagawa, K., Koike, T., 2016. Evaluation of cultivation environment and management based on LAI measurement in farmers' paddy fields in Pursat province. Cambodia. Field Crops Res. 199, 150–155. https://doi.org/10.1016/j.fcr.2016.08.031.

Homma, K., Horie, T., 2009. The present situation and the futureimprovement of fertilizer applicationsby farmers in rainfed rice culture. In: Elsworth, L.R., Paley, W. O. (Eds.), Fertilizers: Properties, Applications and Effects. Nova Science Publishers Inc, New York, NY, pp. 147–180.

Homma, K., Horie, T., Shiraiwa, T., Sripodok, S., Supapoj, N., 2004. Delay of heading date as an index of water stress in rainfed rice in mini-watersheds in Northeast Thailand. Field Crops Res. 88, 11–19. https://doi.org/10.1016/j.fcr.2003.08.010.

Homma, K., Koike, T., Tsujimoto, K., Ohta, T., 2017a. Climate change impact on rice production in Musi river basin in Indonesia. J. Earth Sci. Clim. Change 8, 31. https://doi.org/10.4172/2157-7617-C1-036.

Homma, K., Maki, M., Hirooka, Y., 2017b. Development of a rice simulation model for remote-sensing (SIMRIW-RS). J. Agric. Meteorol. 73, 9–15. https://doi.org/10.2480/agrmet.d-14-00022.

Horie, T., Nakagawa, H., Centeno, H., Kropff, M., 1995. The rice crop simulation model SIMRIW and its testing. In: Matthews, R.B., Kropff, M.J., Bachelet, D., van Laar, H.H. (Eds.), Modeling the Impact of Climate Change On Rice Production. CAB International, AsiaOxon, U.K., pp. 51–66

Horie, T., Yajima, M., Nakagawa, H., 1992. Yield forecasting. Agric. Syst. 40, 211–236. https://doi.org/10.1016/0308-521x(92)90022-g.

Hou, A.Y., Kakar, R.K., Neeck, S., Azarbarzin, A.A., Kummerow, C.D., Kojima, M., Oki, R., Nakamura, K., Iguchi, T., 2014. The global precipitation measurement mission. Bull. Am. Meteorol. Soc. 95, 701–722. https://doi.org/10.1175/bams-D-13-00164.1.

IPCC, 2014. Climate Change 2014 Synthesis Report. IPCC, Geneva, Switzerland.

Iwahashi, Y., Ye, R., Kobayashi, S., Yagura, K., Hor, S., Soben, K., Homma, K., 2021. Quantification of changes in rice production for 2003–2019 with MODIS LAI Data in Pursat Province. Cambodia. Remote Sens. 13, 1971. https://doi.org/10.3390/rs13101971.

Jones, J.W., Tsuji, G.Y., Hoogenboom, G., Hunt, L.A., Thornton, P.K., Wilkens, P.W., Imamura, D.T., Bowen, W.T., Singh, U., 1998. Decision support system for agrotechnology transfer: DSSAT v3. In: Tsuji, G.Y., Hoogenboom, G., Thornton, P.K. (Eds.), Understanding Options for Agricultural Production. Springer Netherlands, Dordrecht, pp. 157–177.

Kawasaki, A., Yamamoto, A., Koudelova, P., Acierto, R., Nemoto, T., Kitsuregawa, M., Koike, T., 2017. Data integration and analysis system (DIAS) contributing to climate change analysis and disaster risk reduction. Data Sci. J. 16, 41. https://doi.org/10.5334/dsj-2017-041.

Kim, H.Y., Lieffering, M., Kobayashi, K., Okada, M., Miura, S.H.U., 2003. Seasonal changes in the effects of elevated CO_2 on rice at three levels of nitrogen supply: a free

air CO_2 enrichment (FACE) experiment. Glob. Change Biol. 9, 826–837. https://doi.org/10.1046/j.1365-2486.2003.00641.x.
Kimball, B.A., Kobayashi, K., Bindi, M., 2002. Responses of agricultural crops to free-air CO_2 enrichment. In: Sparks, D.L. (Ed.), Advances in Agronomy. Academic Press, London, UK, pp. 293–368.
Kobayashi, S., Ota, Y., Harada, Y., Ebita, A., Moriya, M., Onoda, H., Onogi, K., Kamahori, H., Kobayashi, C., Endo, H., Miyaoka, K., Takahashi, K., 2015. The JRA-55 reanalysis: general specifications and basic characteristics. J. Meteorol. Soc. Jpn. II 93, 5–48. https://doi.org/10.2151/jmsj.2015-001.
Kodo, T., Homma, K., Kobayashi, S., Yagura, K., Hor, S., Kim, S., 2021. Effects of irrigation facilities development on cultivation management and productivity of rice in Cambodia: implications based on comparison of adjacent irrigated and nonirrigated areas in Pursat. Jpn. J. Southeast Asian Stud. 59, 101–118. https://doi.org/10.20495/tak.59.1_101.
Krishnan, P., Swain, D.K., Bhaskar, B.C., Nayak, S.K., Dash, R.N., 2007. Impact of elevated CO2 and temperature on rice yield and methods of adaptation as evaluated by crop simulation studies. Agric. Ecosyst. Environ. 122, 233–242. https://doi.org/10.1016/j.agee.2007.01.019.
Li, S., Wang, Q., Chun, J.A., 2017. Impact assessment of climate change on rice productivity in the Indochinese Peninsula using a regional-scale crop model. Int. J. Climatol. 37, 1147–1160. https://doi.org/10.1002/joc.5072.
Mahmood, R., 1998. Air temperature variations and rice productivity in Bangladesh: a comparative study of the performance of the YIELD and the CERES-Rice models. Ecol. Model. 106, 201–212. https://doi.org/10.1016/s0304-3800(97)00192-0.
Maki, M., Sekiguchi, K., Homma, K., Hirooka, Y., Oki, K., 2017. Estimation of rice yield by SIMRIW-RS, a model that integrates remote sensing data into a crop growth model. J. Agric. Meteorol. 73, 2–8. https://doi.org/10.2480/agrmet.D-14-00023.
Masumoto, T., Yoshida, T., Kudo, R., 2016. Basin-scale irrigation planning in areas with scarce data. Irrig. Drain. 65, 22–30. https://doi.org/10.1002/ird.2032.
McLaughlin, D., Kinzelbach, W., 2015. Food security and sustainable resource management. Water Resour. Res. 51, 4966–4985. https://doi.org/10.1002/2015wr017053.
Mekong River Commission, 2018. Irrigation Database Improvement For the Lower Mekong Basin. MRC Technical Report No. 1. Mekong River Commission, Vientiane, Laos.
NASA, 2020. ASTER Global Digital Elevation Map Announcement. NASA, Washington, DC.
National Climatic Change Committe, 2013. Cambodia Climate Change Strategic Plan 2014-2023. National Climatic Change Committe, Cambodia.
Nyunt, C.T., Koike, T., Yamamoto, A., 2016. Statistical bias correction for climate change impact on the basin scale precipitation in Sri Lanka, Philippines, Japan and Tunisia. Hydrol. Earth Syst. Sci. Discuss. 1–32. https://doi.org/10.5194/hess-2016-14.
Ohnishi, M., Horie, T., Koroda, Y., 1997. Simulating rice leaf area development and dry matter production in relation to plant N and weather. In: Kropff, M., Teng, P., Aggarwal, P., Bouma, J., Bouman, B., Jones, J., Van Laar, H. (Eds.), Applications of Systems Approaches At the Field Level. Springer, Netherlands, pp. 271–284.
Prabnakorn, S., Maskey, S., Suryadi, F.X., de Fraiture, C., 2018. Rice yield in response to climate trends and drought index in the Mun River Basin. Thailand. Sci. Total Environ. 621, 108–119. https://doi.org/10.1016/j.scitotenv.2017.11.136.
Prasad, P.V.V., Boote, K.J., Allen, L.H., Sheehy, J.E., Thomas, J.M.G., 2006. Species, ecotype and cultivar differences in spikelet fertility and harvest index of rice in response to high temperature stress. Field Crops Res. 95, 398–411. https://doi.org/10.1016/j.fcr.2005.04.008.
Raksapatcharawong, M., Veerakachen, W., Homma, K., Maki, M., Oki, K., 2020. Satellite-based drought impact assessment on rice yield in Thailand with SIMRIW− RS. Remote Sens. 12, 2099. https://doi.org/10.3390/rs12132099.
Richards, L.A., 1931. Capillary conduction of liquids through porous mediums. Physics (College Park Md) 1, 318–333. https://doi.org/10.1063/1.1745010.
Ruan, Y., Yao, Z., Wang, R., Liu, Z., 2018. Ranking of CMIP5 GCM Skills in simulating observed precipitation over the lower mekong basin, using an improved score-based method. Water (Basel) 10, 1868. https://doi.org/10.3390/w10121868.
Saseendran, S.A., Singh, K.K., Rathore, L.S., Singh, S.V., Sinha, S.K., 2000. Effects of climate change on rice production in the tropical humid climate of Kerala, India. Clim. Change 44, 495–514. https://doi.org/10.1023/a:1005542414134.
Sellers, P.J., Randall, D.A., Collatz, G.J., Berry, J.A., Field, C.B., Dazlich, D.A., Zhang, C., Collelo, G.D., Bounoua, L., 1996. A revised land surface parameterization (SiB2) for atmospheric GCMS. Part I: model formulation. J. Clim. 9, 676–705 https://doi.org/10.1175/1520-0442(1996)009<0676:arlspf>2.0.co;2.
So Im, M., Tsujimoto, K., Aida, K., Tamagawa, K., Ohta, T., Koike, T., Nukui, T., Sobue, S. I., Homma, K., 2014. Water and food security under climate change in Cambodia. Trans. Jpn. Soc. Aeronaut. Space Sci. Aerosp. Technol. Jpn. 12. Tn_31-Tn_39. https://doi.org/10.2322/tastj.12.tn_31.
Steduto, P., Hsiao, T.C., Raes, D., Fereres, E., 2009. AquaCrop-The FAO crop model to simulate yield response to water: I. Concepts and underlying principles. Agron. J. 101, 426–437. https://doi.org/10.2134/agronj2008.0139s.
Sun, F., Mejia, A., Zeng, P., Che, Y., 2019. Projecting meteorological, hydrological and agricultural droughts for the Yangtze River basin. Sci. Total Environ. 696, 134076 https://doi.org/10.1016/j.scitotenv.2019.134076.
Taylor, K.E., Stouffer, R.J., Meehl, G.A., 2012. An overview of CMIP5 and the experiment design. Bull. Am. Meteorol. Soc. 93, 485–498. https://doi.org/10.1175/bams-D-11-00094.1.
Tsujimoto, K., Masumoto, T., Mitsuno, T., 2008. Seasonal changes in radiation and evaporation implied from the diurnal distribution of rainfall in the Lower Mekong. Hydrol. Process. 22, 1257–1266. https://doi.org/10.1002/hyp.6935.
Tsujimoto, K., Ohta, T., Aida, K., Tamakawa, K., So Im, M., 2018. Diurnal pattern of rainfall in Cambodia: its regional characteristics and local circulation. Prog. Earth Planet. Sci. 5, 39. https://doi.org/10.1186/s40645-018-0192-7.
Tsujimoto, K., Ohta, T., Hirooka, Y., Homma, K., 2019. Estimation of planting date in paddy fields by time-series MODIS data for basin-scale rice production modeling. Paddy Water Environ. 17, 83–90. https://doi.org/10.1007/s10333-019-00700-x.
Tsujimoto, K., Ono, K., Ohta, T., Chea, K., Muth, E.N., Hor, S., Hok, L., 2021. Multiyear analysis of the dependency of the planting date on rainfall and soil moisture in paddy fields in Cambodia, 2003–2019. Paddy Water Environ. 19, 635–648. https://doi.org/10.1007/s10333-021-00863-6.
USGS, 2020a. Global Land Cover Characterization (GLCC). Version 1.2. USGS, Reston, Virginia.
USGS, 2020b. MODIS/Aqua Vegetation Indices 16-day L3 Global 250m SIN Grid. USGS, Reston, Virginia.
USGS, 2020c. MODIS/Terra Vegetation Indices 16-day L3 Global 250m SIN Grid. USGS, Reston, Virginia.
USGS, 2020d MODIS/Terra+Aqua Leaf Area Index/FPAR 8-Day L4 Global 500m SIN Grid. USGS, Reston, Virginia.
van Genuchten, M.T., 1980. A closed-form equation for predicting the hydraulic conductivity of unsaturated soils. Soil Sci. Soc. Am. J. 44, 892–898. https://doi.org/10.2136/sssaj1980.03615995004400050002x.
Wang, L., Koike, T., Yang, K., Jackson, T.J., Bindlish, R., Yang, D., 2009b. Development of a distributed biosphere hydrological model and its evaluation with the Southern Great Plains Experiments (SGP97 and SGP99). J. Geophys. Res. 114, D08107. https://doi.org/10.1029/2008jd010800.
Wang, L.E.I., Koike, T., Yang, D., Yang, K.U.N., 2009a. Improving the hydrology of the Simple Biosphere Model 2 and its evaluation within the framework of a distributed hydrological model. Hydrol. Sci. J. 54, 989–1006. https://doi.org/10.1623/hysj.54.6.989.
Yang, D., Herath, S., Musiake, K., 2002. A hillslope-based hydrological model using catchment area and width functions. Hydrol. Sci. J. 47, 49–65. https://doi.org/10.1080/02626660209492907.
Yatagai, A., Kamiguchi, K., Arakawa, O., Hamada, A., Yasutomi, N., Kitoh, A., 2012. APHRODITE: constructing a long-term daily gridded precipitation dataset for Asia based on a dense network of rain gauges. Bull. Am. Meteorol. Soc. 93, 1401–1415. https://doi.org/10.1175/bams-D-11-00122.1.
Zhang, H., Zhou, G., Liu, D.L., Wang, B., Xiao, D., He, L., 2019a. Climate-associated rice yield change in the Northeast China Plain: a simulation analysis based on CMIP5 multi-model ensemble projection. Sci. Total Environ. 666, 126–138. https://doi.org/10.1016/j.scitotenv.2019.01.415.
Zhang, W., Zhou, T., Zhang, L., Zou, L., 2019b. Future intensification of the water cycle with an enhanced annual cycle over global land monsoon regions. J. Clim. 32, 5437–5452. https://doi.org/10.1175/jcli-D-18-0628.1.
Zheng, J., Wang, W., Ding, Y., Liu, G., Xing, W., Cao, X., Chen, D., 2020. Assessment of climate change impact on the water footprint in rice production: historical simulation and future projections at two representative rice cropping sites of China. Sci. Total Environ. 709, 136190 https://doi.org/10.1016/j.scitotenv.2019.136190.